

Amyloid Protofibril is Highly Voluminous and Compressible[†]Kazuyuki Akasaka,^{*,‡} Abdul Raziq Abdul Latif,^{‡,‡} Akihiro Nakamura,[§] Koichi Matsuo,[§] Hideki Tachibana,^{||} and Kunihiro Gekko[§]

Department of Biotechnological Science, School of Biology-Oriented Science and Technology, Kinki University, 930 Nishimitani, Kinokawa, Wakayama 649-6493, Japan, Department of Mathematical and Life Sciences, Graduate School of Science, Hiroshima University, 1-3-1 Kagamiyama, Higashi-Hiroshima, Hiroshima 739-8526, Japan, and Department of Biology, Graduate School of Science, Kobe University, 1-1 Rokkodai-cho, Kobe, Hyogo 657-8501, Japan

Received April 8, 2007; Revised Manuscript Received July 10, 2007

ABSTRACT: We report here results of the first direct measurement of partial volume and compressibility changes of a protein as it forms an amyloid protofibril. We use a high precision density meter and an ultrasonic velocity meter on a solution of intrinsically denatured, disulfide-deficient variant of hen lysozyme, and follow the time-dependent changes in volume and compressibility, as the protein spontaneously forms a protofibril. We have found a large increase in partial specific volume with time from 0.684 to 0.724 mL·g⁻¹ ($\Delta v = 0.040$ mL·g⁻¹ corresponding to 570 mL·(mol monomer)⁻¹) and in partial specific adiabatic compressibility coefficient from -7.48×10^{-12} to $+1.35 \times 10^{-12}$ cm²·dyn⁻¹ ($\Delta\beta_s = 8.83 \times 10^{-12}$ ·cm²·dyn⁻¹) as the monomer transforms into a protofibril. The results demonstrate that the protofibril is a highly voluminous and compressible entity, disclosing a cavity-rich, fluctuating nature for the amyloid protofibril. The volume and compressibility changes occur in two phases, the faster one preceding the major development of the β -structure in the protofibril as monitored by CD.

The volume and compressibility of proteins are basic thermodynamic quantities that are closely related to protein hydration (1), cavity formation, dynamics in the folded state (2, 3) and the conformation of the unfolded state (4–7). It is generally accepted that the partial volume of a globular protein decreases as the conformational order or degree of folding decreases (8, 9). Very little is known, however, about how the volume and compressibility would change upon the formation of amyloid fibrils or protofibrils. These parameters are unique in elucidating basic properties of amyloid fibrils concerning compactness, fluctuation, cavities, and hydration, but no direct measurements of these parameters upon forming fibrils have so far been reported, except for the case of monitoring time course of aggregation with various volumetric parameters (10, 11). Moreover, the knowledge on their changes with amyloid protofibril formation will directly answer the question whether the amyloid fibril is dissociated by pressure and how easily it is (12–15).

Protofibrils made from the genetically engineered disulfide-deficient variant of hen lysozyme (OSS¹), in which the eight Cys residues are replaced by Ala or Ser, constitutes an ideal system for such a study (16). It has no tertiary structure as judged from CD, fluorescence, and NMR and may only have residual secondary structure such as nascent helices since it has a far-UV CD band which is somewhat more negative than that in the case of complete chemical denaturation. Namely, the variant is intrinsically almost fully denatured in its monomeric state in the absence of denaturants. It spontaneously forms in mildly acidic solution under mild ionic strength a molecular assembly rich in β -structure (17), which on AFM image reveals itself as protoprotofibrils consisting of a linear array of protein molecules (18). The length of the protofibril varies widely with its population obeying nearly an exponentially decaying function of length, showing that the fibrils grow mainly through the linear polymerization mechanism, namely, by a monomer addition to a growing end of the polymer with a constant affinity (19). In no case were bundles of protofibrils (or a matured amyloid fiber) found that complicate the kinetics.

These protofibrils are dissociated at high pressure in the kbar range and reassociate by lowering pressure in a fully reversible manner (18), suggesting an increase in volume (a positive Δv) upon the formation of protofibril from its monomeric counterpart. A thermodynamic analysis based on pressure-dependent two-dimensional NMR cross-peak intensities gave the value of $\Delta v \sim 100$ mL·(mol monomer)⁻¹ (17, 19). In addition, the kinetic analysis of the pressure

[†] This work was supported by a Grant-in-Aid for Scientific Research No. 17570132 (to H.T.) and a Grant-in-Aid for Scientific Research in Priority Area No. 18031040 (to K.A.) from the Ministry of Education, Culture, Sports, Science and Technology of Japan, and in part by a Grant-in-Aid for the BSE Control Project from the Ministry of Agriculture, Forestry and Fisheries of Japan. The research was conducted under JSPS Core-to-Core Program Action Initiative No. 17009. Abdul Latif was a recipient of a JSPS postdoctoral fellowship for foreign researchers.

* Corresponding author. Tel: +81-736-77-3888. Fax: +81-736-77-4754. E-mail: akasaka@waka.kindai.ac.jp.

[‡] Kinki University.

[§] Hiroshima University.

^{||} Kobe University.

[‡] Present address: Department of Science, Faculty of Education, Sudan University for Science and Technology, Almugran, Alkhartoum, Sudan.

¹ Abbreviations: WT, wild-type; OSS, the disulfide-deficient variant of hen lysozyme; CD, circular dichroism; v , partial specific volume; κ_s , partial specific adiabatic compressibility; β_s , partial specific adiabatic compressibility coefficient.

dissociation reaction using the pressure-jump fluorescence spectroscopy (19) gave a negative activation volume ($\Delta v^\ddagger = -50.5 \text{ mL} \cdot (\text{mol monomer})^{-1}$ at 1 bar) and a negative activation compressibility ($\Delta \kappa^\ddagger = -0.013 \text{ mL} \cdot (\text{mol monomer})^{-1} \cdot \text{bar}^{-1}$), showing that the protofibril in its ground state is more voluminous and compressible than in the activated state. All these results point to a notion that the protofibril is a highly compressible high-volume state. The proof of this notion should come from a direct measurement of volume and compressibility performed both on the monomeric and protofibril state under the same conditions as those described above (in 20 mM sodium acetate buffer and 30 mM sodium chloride at pH 4.0 at 25 °C).

We report here the results of the direct measurement of volume and compressibility changes of the OSS solution as the monomeric OSS molecules assemble into protofibrils on a high-precision density meter and an ultrasonic velocity meter with a protein concentration of 5 $\text{mg} \cdot \text{mL}^{-1}$ in 20 mM sodium acetate buffer and 30 mM sodium chloride at pH 4.0 at 25 °C. Simultaneously, we monitored changes in secondary structure with time using circular dichroism (CD). The simultaneous recording of volumetric parameters and secondary structure assures us that changes in volumetric parameters are due to the monomer-to-Protofibril transition. Since the measurement is made continuously under the same solution condition, it gives directly the difference in volume and compressibility between the monomeric state (at the start of the reaction) and the protofibril state (after the reaction is nearly complete). Such measurements are rare because conformational transitions (such as folding and unfolding) are usually too rapid to allow time-dependent measurements. Instead, the comparison of volume and compressibility of a protein between different conformational states is often made under different solution conditions (e.g., addition of denaturants), which may obscure the validity of the comparison of their volumetric parameters.

The present study provides the first direct comprehensive determination of changes in equilibrium volumetric parameters for a monomer-to-Protofibril transition, a crucial step in the amyloid fibril formation. The result shows surprisingly large increases in both volume and compressibility upon formation of protofibrils, disclosing the peculiar volumetric nature of an amyloid protofibril state.

MATERIALS AND METHODS

Preparation of Matured Protofibrils of OSS. A genetically engineered disulfide-deficient variant of OSS was prepared as described (16). Protofibrils were formed similarly as described previously (19); the freeze-dried OSS powder was first dissolved in pure water to avoid precipitation, and the polymerization reaction was started by mixing the solution with sodium acetate buffer and sodium chloride solution to give a final protein concentration of 5 $\text{mg} \cdot \text{mL}^{-1}$ in 20 mM sodium acetate buffer containing 30 mM sodium chloride at pH 4.0. The concentration of OSS was determined spectrophotometrically by assuming the same extinction coefficient, 23.7 $\text{dL} \cdot (\text{g} \cdot \text{cm})^{-1}$ at 280 nm, as that reported for the reduced form of WT hen lysozyme (20) since all of the aromatic amino acid residues are retained in OSS, and the secondary and tertiary structural characteristics are very similar between

the monomeric states of OSS and the reduced WT hen lysozyme (16, 17; this study). The extinction coefficient may be correspondingly higher for OSS since its molecular weight, 14,196, including its amino-terminally attached methionine residues, is lower by 0.7% compared to that of WT hen lysozyme. This error will cause the decrease of 0.002 $\text{mL} \cdot \text{g}^{-1}$ in absolute value of partial specific volume, which is comparable with an experimental error of density measurements. Then the result will not influence the conclusion of the present work, particularly concerning the difference between the monomer and protofibril states. A total of 2 mL of the OSS solution was then degassed under vacuum for a short time, about 1 mL each of which was introduced into the sample cells for density and sound velocity measurements within 8 min after the self-association started. A drop of the sample solution was also introduced into the optical cell for CD measurements. The reference solvent was prepared by mixing water with sodium acetate buffer and sodium chloride solutions to the same composition as that of the protein solution on a balance to an accuracy of 10^{-5} g.

Density Measurements. The densities of the solvent, ρ_0 , and the OSS solution, ρ , were measured with an accuracy of $1 \times 10^{-6} \text{ g} \cdot \text{mL}^{-1}$ using a precision density meter (DMA5000, Anton Paar, Austria). The temperature of the sample cell was maintained at 25 °C with a high precision Peltier temperature control system. The time dependent change in density of the OSS solution was monitored continuously for 8–1,460 min after starting the fibril formation. Drifts of the density meter and temperature were confirmed negligible from the densities of solvent before and after a series of density measurements of the protein solution. The partial specific volume, v , of the OSS solution at each measuring time was calculated with the following equation:

$$v = (1/c)[(1 - (\rho - c)/\rho_0)] \quad (1)$$

where c is the protein concentration in grams per milliliter of solution. Here, the partial specific volume determined at a fixed protein concentration (5.07 $\text{mg} \cdot \text{mL}^{-1}$) may be regarded as that at infinite dilution of the protein solution since the concentration dependence of the partial specific volume is very small (2, 3).

Ultrasonic Velocity Measurements. The ultrasonic velocities of the solvent, u_0 , and the OSS solution, u , were measured with an accuracy of 0.1 cm/s by means of a high-resolution ultrasonic spectrometer (HR-US 102, Ultrasonic Scientific, Ireland) at a frequency of 5 MHz and 25 °C. About 1 mL of the OSS solution and the solvent was introduced into the two-separated glass cells equipped with the spectrometer, and the time course of the ultrasonic velocity difference between the sample solution and solvent was measured continuously for 8–1,460 min after starting fibril formation. The adiabatic compressibility coefficients of the solvent and the sample solution (β_0 and β) were calculated from the ultrasonic velocity (u_0 and u) and density data (ρ_0 and ρ) at an identical measuring time by using the Laplace equation: $\beta = 1/\rho u^2$. The partial specific adiabatic compressibility coefficient, β_s , of the OSS amyloid protofibril was calculated with eq 2:

$$\beta_s = -(1/v)(\partial v / \partial P) = (\beta_0/cv) [\beta/\beta_0 - (\rho - c)/\rho_0] \quad (2)$$

where P is the pressure.

Circular Dichroism Measurements. An aliquot of the OSS solution used for the volume and compressibility measurements was taken to monitor the progress of the protofibril-forming reaction with time using a CD spectropolarimeter (J-720W, Jasco). To allow a reliable long-time CD monitoring of the OSS solution at the high protein concentration ($5 \text{ mg}\cdot\text{mL}^{-1}$), an assembled-type MgF_2 optical cell, specially constructed for vacuum ultraviolet CD measurements under high vacuum (21), was employed by adjusting the path length to $46 \mu\text{m}$ with a Teflon spacer. As the construction of the cell does not allow an independent temperature control of the sample solution, CD measurements were performed at the temperature of the room ($20 \text{ }^\circ\text{C}$). To protect the protein from possible photodegradation, the UV light was cut off when the spectra were not measured. The time course of the molar ellipticity at 215 nm , $[\theta]_{215}$, was measured continuously for 13–1,614 min after starting fibril formation. To check if the temperature ($20 \text{ }^\circ\text{C}$), different from that ($25 \text{ }^\circ\text{C}$) for volume and compressibility measurements, affected the reaction rate significantly, an additional experiment was performed to monitor the CD spectral change at $25 \text{ }^\circ\text{C}$ on a Jasco J-820 spectropolarimeter equipped with a water-jacketed temperature control cell with a path length of $100 \mu\text{m}$.

Kinetic Analysis of Fibril Formation. The exact analytical formula that describes the time course of nucleation-dependent monomer-addition type association has been derived only under simplifying assumptions (22). Moreover, our previous observation suggested that polymer–polymer addition also takes place in fibril formation (18). Therefore, the time courses of ν , β_s , and $[\theta]_{215}$ were fit here to a double-exponential function of time:

$$X^t = X^\infty - A_1 \exp(-k_1 t) - A_2 \exp(-k_2 t) \quad (3)$$

where X^t and X^∞ are the values of ν , β_s , and $[\theta]_{215}$ at times t and infinity, respectively; A and k are the amplitude and rate-constant of each phase; and subscripts 1 and 2 indicate the fast and slow reaction phases, respectively. However, in the limited experimental time range, fitting the experimental values to eq 3 did not give a good conversion in X^∞ . Therefore, X^∞ values were conventionally taken as the values at $t = 1,460 \text{ min}$ for ν and β_s and as the value at $t = 1,614 \text{ min}$ for $[\theta]_{215}$ after starting fibril formation.

RESULTS

Circular Dichroism (CD) Change Associated with Monomer-to-Fibril Transition. The time dependent monomer-to-protofibril transition of OSS, monitored by CD at pH 4 and $20 \text{ }^\circ\text{C}$ is shown in the inset of Figure 1. The OSS CD spectrum at the initial stage of the transition (13 min) is similar to the CD spectrum observed for the totally reduced and carboxamidomethylated WT hen lysozyme at pH 2 (23). The ellipticity becomes more negative with time with a clear isoellipticity point at 206 nm , and a new peak appears around 215 nm , characteristic of a β -rich amyloid protofibril. The molar ellipticity at 215 nm , $[\theta]_{215}$, changes exponentially with time, and protofibril formation is essentially complete at $1,500 \text{ min}$. A two-phase analysis using eq 3 with the $[\theta]_{215}^\infty$ value of $-11.3 \times 10^3 \text{ deg}\cdot\text{cm}^2\cdot\text{dmol}^{-1}$ gave no significant difference between rate constants k_1 and k_2 . Therefore, the time course of $[\theta]_{215}$ was analyzed with single phase

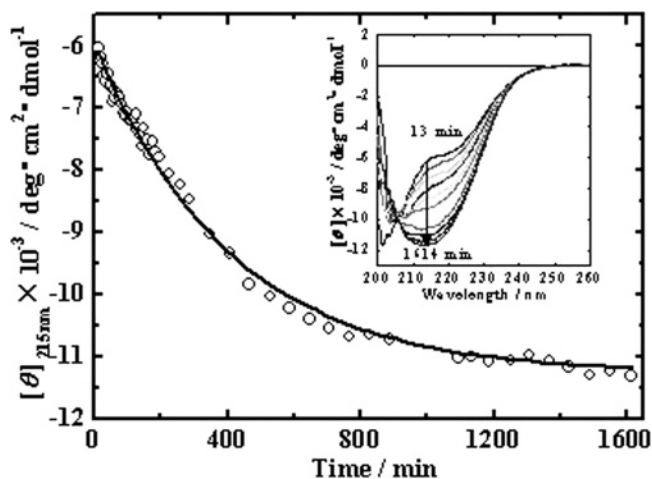


FIGURE 1: Time dependence of the molar ellipticity at 215 nm of OSS during the monomer-to-protofibril transition at $20 \text{ }^\circ\text{C}$. The protein concentration is $5.07 \text{ mg}\cdot\text{mL}^{-1}$ in 20 mM sodium acetate buffer containing 30 mM NaCl (pH 4.0). The solid line is a fitting curve calculated for a single phase transition with the kinetic parameters listed in Table 1. Inset: far-UV CD spectra at 13 (top), 47, 107, 196, 287, 347, 467, 587, 887, 1187, and 1614 min (bottom). Similar data were obtained at $25 \text{ }^\circ\text{C}$.

transition kinetics, giving the fitted curve in Figure 1 with the kinetic parameters listed in Table 1. The CD spectral change monitored at $25 \text{ }^\circ\text{C}$ at a protein concentration of $4.69 \text{ mg}\cdot\text{mL}^{-1}$ also showed single phase kinetics similar to that of Figure 1 with a rate constant of 0.0023 min^{-1} , close to that (0.0025 min^{-1}) at $20 \text{ }^\circ\text{C}$ (data not shown). Obviously, the temperature effect on the rate constant is small.

Density and Volume Changes Associated with Monomer-to-Fibril Transition. Figure 2A shows the time dependent change of the density of the OSS solution during the monomer-to-protofibril transition. The decrease is associated with an increase in partial specific volume. Fitting the experimental data to eq 3 with a ν^∞ value of $0.724 \text{ mL}\cdot\text{g}^{-1}$ (Figure 2A) gives the kinetic parameters listed in Table 1. The partial specific volume of the OSS monomer, $\nu^0 = 0.684 \text{ mL}\cdot\text{g}^{-1}$, is obtained by extrapolating the regression curve to $t = 0$ (at the time of mixing of the OSS aqueous solution and the buffer). The small ν^0 value indicates that the OSS monomer is in an intrinsically denatured state with considerable hydration before the onset of the fibril-forming reaction. The ν^0 value is close to the ν value of $0.682 \text{ mL}\cdot\text{g}^{-1}$ of reduced and acid-denatured carboxamidomethylated WT hen lysozyme at pH 2 (6), which should essentially be in the same conformational state as that of OSS. A separate density measurement of OSS in pure water (stable monomer) also gave a close ν^0 value of $0.680 \text{ mL}\cdot\text{g}^{-1}$ (data not shown). These results are taken to indicate the reliability of ν^0 kinetically obtained for the partial specific volume of the OSS monomer.

The increase in volume for the monomer-to-protofibril transition is $\Delta\nu = \nu^\infty - \nu^0 = 0.724 - 0.684 = 0.040 \text{ mL}\cdot\text{g}^{-1}$, corresponding to $570 \text{ mL}\cdot(\text{mol monomer})^{-1}$. The value is surprisingly large compared to the value of $\Delta\nu$ ($\sim 100 \text{ mL}\cdot(\text{mol monomer})^{-1}$), previously determined from the pressure-dependent equilibrium analysis of the OSS system in 90% $\text{H}_2\text{O}/10\% \text{ D}_2\text{O}$ (v/v) containing 50 mM deuterated sodium maleate buffer at pH 2.0 at $20 \text{ }^\circ\text{C}$, using $^{15}\text{N}/^1\text{H}$ two-dimensional NMR spectra ($7.6 \text{ mg}\cdot\text{mL}^{-1}$) (17, 19). The

Table 1: Kinetic Parameters for the Monomer-to-Protofibril Transition of OSS Obtained from Changes in Molar Ellipticity at 215 nm [θ]₂₁₅, Partial Specific Volume ν , and Adiabatic Compressibility Coefficient β_s^a

	X^0	X^∞	A_1	A_2	k_1 (min ⁻¹)	k_2 (min ⁻¹)
$[\theta]$ (10 ³ ·deg·cm ² ·dmol ⁻¹)	-5.93 ± 0.04	-11.3	-5.37 ± 0.04		0.0025 ± 0.0001	
ν (mL·g ⁻¹)	0.6841 ± 0.0002	0.724	0.0304 ± 0.0003	0.0095 ± 0.0003	0.0127 ± 0.0002	0.0018 ± 0.0001
β_s (10 ⁻¹² ·cm ² ·dyn ⁻¹)	-7.48 ± 0.03	1.35	4.77 ± 0.04	4.06 ± 0.05	0.0145 ± 0.0003	0.0021 ± 0.0001

^a The reaction was carried out at a protein concentration of 5.07 mg·mL⁻¹ in 20 mM sodium acetate buffer (pH 4.0) containing 30 mM sodium chloride at 25 °C. The time course of molar ellipticity was analyzed at 20 °C by assuming a single phase transition in eq 3. Attached are the standard errors in statistical analysis.

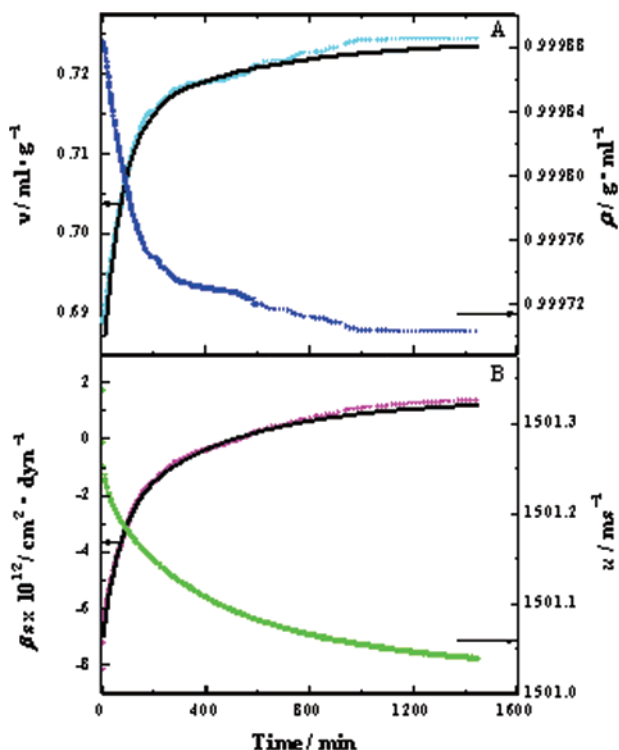


FIGURE 2: Time dependence of the density and partial specific volume (A) and the sound velocity and adiabatic compressibility coefficient (B) of OSS during the monomer-to-protofibril transition at 25 °C. The protein concentration is 5.07 mg·mL⁻¹ in 20 mM sodium acetate buffer containing 30 mM NaCl (pH 4.0). The black solid lines are fitting curves using eq 3 with the kinetic parameters listed in Table 1.

folding of monomeric globular proteins of comparable size usually gives $\Delta\nu \sim 100$ mL·mol⁻¹ (24).

Ultrasonic Velocity and Compressibility Changes Associated with Monomer-to-Fibril Transition. The ultrasonic velocity of the OSS solution, u , decreases during the time course of the monomer-to-protofibril transition (Figure 2B). The decrease is associated with an increase in the partial specific adiabatic compressibility coefficient, β_s . Fitting the experimental data to eq 3 with a β_s^∞ value of 1.35×10^{-12} cm²·dyn⁻¹ (Figure 2B) gives the kinetic parameters listed in Table 1. The partial specific adiabatic compressibility coefficient of the OSS monomer, $\beta_s^0 = -7.48 \times 10^{-12}$ cm²·dyn⁻¹, obtained by extrapolating the regression curve to $t = 0$ is close to the β_s value (-7.0×10^{-12} cm²·dyn⁻¹) of reduced and carboxamidomethylated WT hen lysozyme at pH 2 (6). This coincidence again indicates that the OSS monomer is intrinsically denatured before the initiation of fibril formation. The compressibility change due to the monomer-to-protofibril transition, $\Delta\kappa_s$, defined as the dif-

ference in the partial specific adiabatic compressibility between the two states, $\Delta\kappa_s = \kappa_s^\infty - \kappa_s^0 = \nu^\infty\beta_s^\infty - \nu^0\beta_s^0$, is 6.10×10^{-12} mL·g⁻¹·cm²·dyn⁻¹ using the values of ν^0 , ν^∞ , β_s^0 , and β_s^∞ obtained above.

The rate constants, k_1 and k_2 , observed for the time course of compressibility change differ by nearly an order of magnitude and are close to those observed for the time course of partial specific volume change. The coincidence indicates that the monomer-to-protofibril transition proceeds in a parallel manner in volume and compressibility. The fast k_1 process observed for the volume and compressibility changes is apparently lacking for the β -structure formation observed for CD. The discrepancy does not arise from the difference in the temperature at which measurements were taken (20 °C for CD and 25 °C for volumetric and compressibility) because the CD measurement at 25 °C gave a rate similar to that at 20 °C. The apparent discrepancy of the kinetics must, therefore, arise from a fundamental difference in sensitivity among the methods used to monitor the reaction to the molecular events in the fast phase.

DISCUSSION

Volume and Compressibility Are Sensitive Probes of Cavity, Hydration, and Dynamics. Volume and compressibility are sensitive to internal atom packing (or cavity) and the solvent accessible surface area (or hydration) of a protein molecule, which regulate the dynamics of a protein molecule in solution (2, 3). The partial specific volume of a protein in water is expressed as the sum of three contributions: the constitutive volume estimated as the sum of the constitutive atomic or group volume (V_c); the volume of the cavity or void in the molecule due to imperfect atomic packing (V_{cav}); and the volume change due to solvation or hydration (ΔV_{sol}) (25).

$$\nu = V_c + V_{cav} + \Delta V_{sol} \quad (4)$$

Since the constitutive atomic volume is assumed to be incompressible, the coefficient of partial specific adiabatic compressibility is mainly determined by the internal cavity and surface hydration (2, 3):

$$\beta_s = -(1/\nu)(\partial\nu/\partial P) = -(1/\nu)[\partial V_{cav}/\partial P + \partial(\Delta V_{sol}/\partial P)] \quad (5)$$

Cavity contributes positively and hydration contributes negatively to ν and β_s ; thus, the experimentally observed β_s can be positive or negative depending on the relative magnitude of the two contributions. Since the constitutive atomic volume does not change in protein refolding and association, the volume and compressibility changes due to

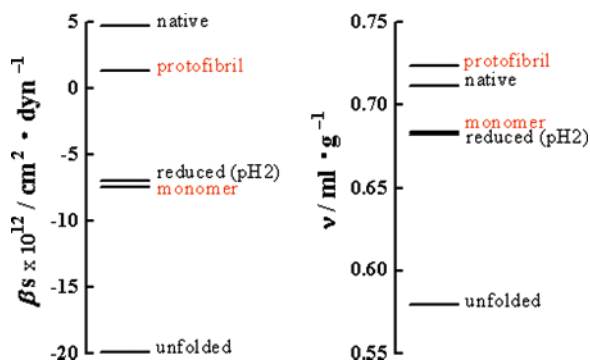


FIGURE 3: Comparison of volume (ν) and adiabatic compressibility coefficient (β_s) levels of OSS (red) and WT hen lysozyme (black) at various conformational states in solution. See text for the solution conditions producing each conformational state.

fibril formation are mainly ascribed to changes in hydration and the cavities.

Protofibril Formation Accompanies a Large Increase in Volume and Compressibility. Figure 3 compares the experimentally determined values of partial specific volume (ν) and partial adiabatic compressibility coefficient (β_s) for the monomeric and protofibril states of OSS with those for WT hen lysozyme at various conformational states in solution obtained from previous measurements (5, 6). The small ν^0 and negative β_s^0 values ($\nu^0 = 0.684 \text{ mL} \cdot \text{g}^{-1}$ and $\beta_s^0 = -7.48 \times 10^{-12} \text{ cm}^2 \cdot \text{dyn}^{-1}$) for the monomer (Table 1 and Figure 3) are consistent with the already established view that the OSS monomer is intrinsically denatured with a considerable degree of hydration, as judged from the CD (Figure 1), NMR (17, 18), and fluorescence (19) spectra as well as from the result of ultracentrifugation (17). Nonetheless, the fact that the β_s^0 value of the OSS monomer ($-7.48 \times 10^{-12} \text{ cm}^2 \cdot \text{dyn}^{-1}$) is considerably larger than the β_s value ($-19.9 \times 10^{-12} \text{ cm}^2 \cdot \text{dyn}^{-1}$) of the WT hen lysozyme fully unfolded by guanidine hydrochloride (5) (Figure 3) indicates that the naturally unfolded OSS monomer has a residual structure excluding full hydration, whereas the guanidinium chloride-treated WT hen lysozyme has almost no residual structure and is fully hydrated. The differences in ν and β_s demonstrate the high sensitivity of volume and compressibility for differentiating hydration states of proteins.

Upon monomer-to-*protofibril* transition, the partial specific volume of OSS increases dramatically from $\nu^0 = 0.684 \text{ mL} \cdot \text{g}^{-1}$ at the start of the transition to $\nu^\infty = 0.724 \text{ mL} \cdot \text{g}^{-1}$ at the final stage of the transition. The latter value is considerably larger even than that of the WT hen lysozyme in its native state ($0.712 \text{ mL} \cdot \text{g}^{-1}$) (2). The result clearly demonstrates that the amyloid *protofibril* of OSS is highly voluminous, even more than that of WT in its folded state, which has a considerable amount of cavities (26). The large volume increase ($\Delta\nu = \nu^\infty - \nu^0 = 0.724 - 0.684 = 0.040 \text{ mL} \cdot \text{g}^{-1}$ or $570 \text{ mL} \cdot (\text{mol monomer})^{-1}$) in the monomer-to-*protofibril* transition is certainly consistent with the earlier finding that the OSS amyloid *protofibril* dissociates at high pressure (17–19). However, the $\Delta\nu$ value kinetically and directly determined from density measurements in the present work ($570 \text{ mL} \cdot (\text{mol monomer})^{-1}$) is far greater than that ($\sim 100 \text{ mL} \cdot (\text{mol monomer})^{-1}$) determined previously from the equilibrium analysis with variable

pressure (17, 19). This discrepancy may arise from two reasons, namely, (1) the transition treated in equilibrium analysis represents part of the total transition, thereby giving a fractional $\Delta\nu$ value rather than the entire volume change, and additionally, (2) the spectroscopically detected signal intensity may not necessarily represent the reactant population correctly.

Upon monomer-to-*protofibril* transition, the compressibility coefficient of OSS also increases dramatically from the negative $\beta_s^0 = -7.48 \times 10^{-12} \text{ cm}^2 \cdot \text{dyn}^{-1}$ at the start of the transition to the positive $\beta_s^\infty = +1.35 \times 10^{-12} \text{ cm}^2 \cdot \text{dyn}^{-1}$ at the final stage of the transition ($\Delta\beta_s = 8.83 \times 10^{-12} \text{ cm}^2 \cdot \text{dyn}^{-1}$). The large negative compressibility of the monomeric state ($\beta_s^0 = -7.48 \times 10^{-12} \text{ cm}^2 \cdot \text{dyn}^{-1}$) is fully consistent with the intrinsically denatured state of the OSS monomer, whereas the increase into positive value ($\beta_s^\infty = +1.35 \times 10^{-12} \text{ cm}^2 \cdot \text{dyn}^{-1}$) indicates that in the *protofibril* state the compressibility is dominated by the cavity effect rather than the hydration effect. Even so, the β_s^∞ value of the *protofibril* is still smaller than β_s of the native WT hen lysozyme ($4.7 \times 10^{-12} \text{ cm}^2 \cdot \text{dyn}^{-1}$) (2). This is probably due to the fact that in the *protofibril* state a considerable portion of the polypeptide chain is still exposed and hydrated; our preliminary hydrogen/deuterium exchange measurements indeed show that more than 70% of the main chain amide groups of OSS are exposed to the solvent in the *protofibril* state (unpublished results). Although it is difficult to partition the contributions of hydration and cavities, we expect that a small increase in the number of cavities will account for the increased compressibility of the *protofibril* since the compressibility of a cavity is about 10 times larger than that of water (2, 3). In summary, the values of $\Delta\beta_s$ and $\Delta\nu$ suggest that the transition of monomers to the *protofibril* is accompanied by an increase in cavity and a decrease in hydration, presumably because of a loss of water in the surface area at the monomer–monomer contact.

The conclusion drawn by Smironovas et al. on polylysine (10) and insulin (11) aggregation and amyloidogenesis that it accompanies a compaction and reduction in the partial specific volume as well as a decrease in compressibility is in apparent contradiction to our present conclusion. However, only temperature dependence was reported in the former case, whereas in the latter case, the protein conformation (a partly unfolded state formed by an endothermic transition) at the start of the association reaction is apparently giving different volumetric properties than those for the present study. Moreover, significant differences exist in the morphology of the product fibrils. In general, a casual extension of the present result to other amyloid systems should be made with caution. For example, pressure does not necessarily lead to the dissociation of amyloid fibrils, as reported in the literature (13, 14). Besides possible kinetic barriers for dissociation due to the size and bundle structures of matured amyloid fibrils, a large volume decrease upon dissociation is not always assured when the monomer is refolded (cf. Figure 3). Clearly, we need more data on fibrillation systems with simple, well defined conformations or structures for both the starting material and the product fibril to generally discuss the trend in volumetric changes upon amyloid fibril formation.

Protofibril Formation Proceeds in Two Phases. While the secondary structure formation represented by the CD spectral change follows a single phase kinetics, the increase in ν and β_s with time (Figure 2) indicates that the monomer-to-protofibril transition proceeds in two phases, fast and slow, with rate constants differing by an order of magnitude. The rate constant 0.0025 min^{-1} for the single phase CD change is rather close to 0.0018 and 0.0021 min^{-1} for the volume and compressibility changes in the slow phase. Although the initial purpose of the CD measurement in the present work was to monitor the progress of the reaction with well established CD spectral changes rather than to compare the kinetic result with those obtained from the volumetric measurements, the clear discrepancy in the apparent kinetics of the reaction is worthy of attention as it might hint at the early event of the reaction.

One obvious possibility for the discrepancy observed in the fast phase of the reaction would be that the initial association of monomers is driven by hydrophobic interactions and that it does not readily develop the ordered β -structure detectable as CD changes, whereas it contributes significantly to the volume and compressibility changes. (About three-quarters of the total volume change and about half of the total compressibility change take place in the fast phase (Table 1).) A supporting evidence for the molecular association occurring before the CD change takes place comes from the preliminary size-exclusion chromatography measurements, which can separately quantitate the polymer fraction and the monomer fraction (data not shown). The analysis gave a single rate constant of 0.0078 min^{-1} for exactly the same experimental condition as that for the volumetric measurements, about three times larger than that for the CD change. Also, the time course of turbidity increase, reflecting an increase in the weight averaged molecular weight (modified by particle dissipation factors), was regressed to a double-exponential function to give the fast phase rate constant of 0.0081 min^{-1} , again much faster than the CD change. Thus, it appears certain that some molecular association process, rather silent to the CD spectral change, takes place in the fast phase, whereas in the slow phase, the major development of the β -structure takes place. The molecular event in the early phase of the association, suggested here, must be delineated in more detail in future works.

In the slow phase, elongation and redistribution of preformed molecular aggregates into protofibrils will take place along with the development of the β -structure. Redistribution can take place mainly through the attachment and detachment of monomers from the end(s) of the polymer (19) but also through end-to-end polymer-polymer association, which has been suggested to take place in the pressure jump NMR study of OSS protofibrils (18). We need further experimental studies on a variety of systems to pursue the underlying principle and the generality of the two-phase transition phenomenon in protofibril formation.

CONCLUDING REMARKS

We have shown that changes in partial specific volume and compressibility associated with the formation of the amyloid protofibril from disulfide-deficient hen lysozyme can be measured with reasonable accuracy. Similar measurements of volume and compressibility changes in

other amyloid systems are expected to open a new horizon of amyloid research because they not only provide a clear basis for judging whether or not the amyloid fibril is dissociable by pressure but also provide, more importantly, information for voids (cavities), hydration, and structural fluctuation, which are crucial for characterizing the dynamics and reactivity of amyloid fibrils. Furthermore, time dependent changes in volume and compressibility could be particularly sensitive to the early event in molecular association and protofibril growth.

ACKNOWLEDGMENT

We thank Yukari Natsukawa for her technical assistance. We also thank Mariko Araga and Ryohei Kono for their collaboration in carrying out additional density and CD measurements.

REFERENCES

- Chalikian, T. V., Sarvazyan, A. P., and Breslauer, K. J. (1994) Hydration and partial compressibility of biological compounds, *Biophys. Chem.* **51**, 89–107.
- Gekko, K., and Noguchi, H. (1979) Compressibility of globular proteins in water at 25 °C. *J. Phys. Chem.* **83**, 2706–2714.
- Gekko, K., and Hasegawa, Y. (1986) Compressibility-structure relationship of globular proteins, *Biochemistry* **25**, 6563–6571.
- Tamura, Y., and Gekko, K. (1995) Compactness of thermally and chemically denatured ribonuclease A as revealed by volume and compressibility, *Biochemistry* **34**, 1878–1884.
- Kamiyama, T., and Gekko, K. (1997). Compressibility and volume changes of lysozyme due to guanidine hydrochloride denaturation, *Chem. Lett.* 1063–1064.
- Gekko, K., Kimoto, A., and Kamiyama, T. (2003) Effects of disulfide bonds on compactness of protein molecules revealed by volume, compressibility, and expansibility changes during reduction, *Biochemistry* **42**, 13746–13753.
- Chalikian, T. V., and Breslauer, K. J. (1996) Compressibility as a means to detect and characterize globular protein states, *Proc. Natl. Acad. Sci. U.S.A.* **93**, 1012–1014.
- Kitahara, R., Yamada, H., Akasaka, K., and Wright, P. E. (2002) High pressure NMR reveals that apomyoglobin is an equilibrium mixture from the native to the unfolded, *J. Mol. Biol.* **320**, 311–319.
- Akasaka, K. (2003) Highly fluctuating protein structures revealed by variable pressure NMR, *Biochemistry* **42**, 1875–1885.
- Smirnovas, V., Winter, R., Funk, T., and Dzwolak, W. (2005) Thermodynamic properties underlying the alpha-to-helix-to-beta-sheet transition, aggregation, and amyloidogenesis of polylysine as probed by calorimetry, densimetry, and ultrasound velocity, *J. Phys. Chem. B* **109**, 19043–19045.
- Smirnovas, V., Winter, R., and Dzwolak, W. (2006) Protein amyloidogenesis in the context of volume fluctuations: a case study of insulin, *ChemPhysChem* **7**, 1046–1049.
- Foguel, D., Suarez, M. C., Ferrao-Gonzales, A. D., Porto, T. C., Palmieri, L., Einsiedler, C. M., Andrade, L. R., Lashuel, H. A., Lansbury, P. T., Kelly, J. W., and Silva, J. L. (2003) Dissociation of amyloid fibrils of alpha-synuclein and transthyretin by pressure reveals their reversible nature and the formation of water-excluded cavities, *Proc. Natl. Acad. Sci. U.S.A.* **100**, 9831–9836.
- Dirix, C., Meersman, F., MacPhee, C. E., Dobson, C. M. and Heremans, K. (2005) High hydrostatic pressure dissociates early aggregates of TTR105-115, but not the mature amyloid fibrils, *J. Mol. Biol.* **347**, 903–909.
- Chatani, E., Kato, M., Kawai, T., Naiki, H., and Goto, Y. (2005) Main-chain dominated amyloid structures demonstrated by the effect of high pressure, *J. Mol. Biol.* **352**, 941–951.
- Meersman, F., and Dobson, C. M. (2006) Probing the pressure-temperature stability of amyloid fibrils provides new insights into their molecular properties, *Biochim. Biophys. Acta* **1764**, 452–460.

16. Tachibana, H. (2000) Propensities for the formation of individual disulfide bonds in hen lysozyme and the size and stability of disulfide-associated submolecular structures, *FEBS Lett.* **480**, 175–178.
17. Niraula, T. N., Konno, T., Li, H., Yamada, H., Akasaka, K., and Tachibana, H. (2004) Pressure-dissociable reversible assembly of intrinsically denatured lysozyme is a precursor for amyloid fibrils, *Proc. Natl. Acad. Sci. U.S.A.* **101**, 4089–4093.
18. Kamatari, Y. O., Yokoyama, S., Tachibana, H., and Akasaka, K. (2005) Pressure-jump NMR study of dissociation and association of amyloid protofibrils, *J. Mol. Biol.* **349**, 916–921.
19. Abdul Latif, A. R., Kono, R., Tachibana, H., and Akasaka, K. (2007) Kinetic analysis of amyloid protofibril dissociation and volumetric properties of the transition state, *Biophys. J.* **92**, 323–329.
20. Saxena, V. P., and Wetlaufer, D. B. (1970) Formation of three-dimensional structure in proteins. I. Rapid nonenzymic reactivation of reduced lysozyme, *Biochemistry* **9**, 5015–5023.
21. Matsuo, K., Sakai, K., Matsushima, Y., Fukuyama, T., and Gekko, K. (2003) Optical cell with a temperature-control unit for a vacuum-ultraviolet circular dichroism spectrophotometer, *Anal. Sci.* **19**, 129–132.
22. Oosawa, F., and Asakura, S. (1975). *Thermodynamics of the Polymerization of Protein*, Academic Press, London.
23. White, H. F., Jr. (1976) Studies on secondary structure in chicken egg-white lysozyme after reductive cleavage of disulfide bond, *Biochemistry* **15**, 2906–2912.
24. Royer, C. A. (2002) Revisiting volume changes in pressure-induced protein unfolding, *Biochim. Biophys. Acta* **1595**, 201–209.
25. Kauzmann, W. (1959) Some factors in the interpretation of protein denaturation, *Adv. Protein Chem.* **14**, 1–63.
26. Diamond, R. (1974) Real-space refinement of the structure of hen egg-white lysozyme, *J. Mol. Biol.* **62**, 371–391.

BI700648B